Gabor deconvolution: surface and subsurface consistent

David C. Henley, Gary F. Margrave and Carlos Montana

ABSTRACT

Nonstationary deconvolution methods are beginning to gain acceptance for routine seismic data processing, possibly in recognition of their ability to correct for the effects of anelastic attenuation. Gabor deconvolution has been introduced as a natural way to accommodate the temporal nonstationarity of seismic traces; and more recently, the underlying model has been extended to directly solve for lateral nonstationarity in the earth in a surface consistent way. The latest Gabor algorithm has recently been implemented as a test module in ProMAX, and it is constructed in such a way as to enable testing of various wavelet and Q function apportionment schemes for the estimation and removal of both surface and sub-surface dependent effects. The module also has the capability to iteratively improve the various wavelet estimates. This report describes the module and its parameters and shows some comparative examples of its output.

INTRODUCTION

The purpose of deconvolution is to extract the highest resolution earth reflectivity function possible from seismic reflection data. Early methods used a single stationary operator applied to individual data traces, where the operator is designed using measured wavelets or statistical characteristics of the data themselves. Later the stationary method was extended in a number of ways, including surface consistent extensions. More recent developments have attempted to account for the influence of known phenomena in the earth in order to design more suitable operators. Among these efforts is the development of Gabor deconvolution, which uses the Gabor transform to estimate, from the data, an array of deconvolution operators which accommodate the nonstationarity of seismic data due to the influence of earth effects like attenuation or absorption (Margrave et al 2001, 2002, 2003).

The influence of the near-surface on deconvolution operators has also been considered recently, since it is known that near-surface coupling, scattering, and other phenomena contribute to variations in seismic response with surface location. The surface-consistent derivation of deconvolution operators has been implemented by a number of investigators, but in general, such operators are stationary in time. Montana et al (2006) introduced a new Gabor deconvolution algorithm which is able to incorporate surface consistency as well as nonstationarity in time.

This report introduces a new version of the Gabor algorithm for ProMAX, which implements the method of Montana et al for testing by sponsors, and also provides a test platform for various schemes for partitioning the deconvolution operator among the various factors thought to influence the seismic recording process.

THE ALGORITHM

The new ProMAX operation, **gabor_sc**, is basically an implementation of the equations and procedures outlined in Montana et al (2006), but there are some enhancements and additional features, which will be described below.

The Montana algorithm

As described in Montana et al (2006), the surface consistent Gabor algorithm operates as follows:

- Storage arrays are established, indexed by source position, receiver position, and midpoint position. The source and receiver storage arrays are one dimensional (frequency) constructs while the midpoint array is two dimensional (time and frequency).

- During the first pass through the entire dataset, each input trace is transformed to the Gabor domain, to obtain a 2D, time-frequency representation.

- Hyperbolic smoothing is applied to the Gabor magnitude spectrum, and the smoothed surface (the Q-array) is summed into the storage array indexed by the midpoint of the current trace.

- The residual magnitude spectrum is estimated by dividing the trace magnitude spectrum by the Q-array and summing the result over time. The square root of the residual magnitude spectrum is summed to the storage array indexed by source position of the current trace.

- The square root of the residual magnitude spectrum is also summed to the storage array indexed by receiver position of the current trace.

- Once all the input traces have been read, the storage arrays are normalized by their respective fold numbers.

- Each input trace is read a second time and transformed once again to Gabor space.

- The magnitude of a time-frequency deconvolution operator for the current trace is assembled by extending the averaged magnitude spectra for the current trace source and receiver positions (from the source and receiver arrays) into constant functions of time, multiplying these together and then multiplying by the Q-array for the current midpoint position.

- The magnitude of the deconvolution operator is stabilized by the addition of a small positive constant (stability factor) and its minimum phase spectrum is calculated using the conventional Kolomogorov algorithm applied at each time.

- The complex-valued Gabor spectrum of the deconvolution operator is divided into the complex-valued Gabor spectrum of the current trace giving the Gabor spectrum of the deconvolved trace.

- The deconvolved trace is reconstructed by inverse Gabor transform and output from the algorithm.

The ProMAX implementation

As written, the new ProMAX process, **gabor_sc**, can be set up to operate just as described above by enabling or disabling a few key lines of code and setting parameters appropriately. However, it has been extended to enable additional flexibility whose utility will be the subject of future research. For readability, we describe the complete extended algorithm below and comment on the differences with the Montana algorithm.

- Two sets of identical storage arrays are established, each set consisting of arrays indexed by source position, receiver position, midpoint position, and absolute offset bin. One set of storage arrays is used for the *current estimate* spectra, and the other for the *iterated estimate* spectra.

- During the first pass through the entire dataset, each input trace is transformed to the Gabor domain, to obtain a 2D, time-frequency representation.

- Hyperbolic smoothing is applied to the trace Gabor magnitude spectrum, and the smoothed surface (Q-array) is summed into the *current estimate* storage array indexed by midpoint.

- The residual magnitude spectrum is estimated by dividing the trace magnitude spectrum by the Q-array, but without summing over time. The cube root of the residual magnitude spectrum is summed into the *current estimate* offset array indexed by the absolute offset of the current trace.

- The cube root of the residual magnitude spectrum is also summed into the *current estimate* source array indexed by source position of the current trace.

- The cube root of the residual magnitude spectrum is additionally summed into the *current estimate* receiver array indexed by receiver position of the current trace.

- After all input traces have been read, all *current estimate* storage arrays are normalized by their respective fold counts. These arrays now contain the *first estimates* for the deconvolution operator components. That is, we have ensemble averages for the Q-array at each midpoint, the offset attenuation function at each offset, the source waveform at each source location, and the receiver waveform at each receiver location. All of these arrays are time and frequency dependent.

- During the second pass, each original raw input trace is again transformed to the Gabor domain.

- The residual trace Gabor magnitude spectrum is re-estimated by dividing the Gabor magnitude spectrum by its hyperbolically smoothed self. (Note that the hyperbolically smoothed trace spectrum is not used again beyond here. Also, it may be useful to do this estimation another way in the future. The residual Gabor magnitude spectrum could also be obtained by dividing the *current* Gabor magnitude spectrum by the accumulated *current estimate* spectrum in the Q-array corresponding to the trace midpoint, for example.)

- The residual trace Gabor magnitude spectrum is divided by the product of its corresponding stored *current estimate* source and *current estimate* receiver magnitude spectra to give a new (iterated) estimate of the *offset* contribution to the current Gabor spectrum. This estimate is summed to the separate *iterated estimate* offset array, indexed by the offset of the current trace. The *current estimate* spectra remain unchanged.

- The residual trace Gabor magnitude spectrum is also divided by the product of its corresponding stored *current estimate* offset and *current estimate* receiver magnitude spectra to give an iterated *source* estimate, which is stored in the *iterated estimate* source array indexed by the source position of the current trace. The *current estimate* spectra remain unchanged.

- The residual trace Gabor magnitude spectrum is additionally divided by the product of its corresponding stored *current estimate* offset and *current estimate* source magnitude spectra to give an iterated *receiver* estimate, which is stored in the *iterated estimate* receiver array indexed by the receiver position of the current trace. The *current estimate* spectra remain unchanged.

- A *current estimate* deconvolution operator is assembled for the current trace by multiplying magnitude spectra retrieved from the *current estimate* arrays corresponding to source, receiver, and offset locations for the current trace and multiplying by the Q-array for the current midpoint location.

- The operator is stabilized by addition of a stability factor and converted (optionally) to minimum phase.

- The complex Gabor spectrum of the current trace is divided by the complex deconvolution operator spectrum.

- The trace is reconstructed from its modified Gabor spectrum and output from the algorithm.

- After all input traces are read for the second time, the *iterated estimate* magnitude spectra arrays are normalized by their respective fold counts.

- To begin the third and all subsequent passes, the *current estimate* magnitude spectra arrays are replaced by the *iterated estimate* magnitude spectra arrays, and the *iterated estimate* arrays are zeroed to prepare them for the next iteration.

- During the third and subsequent passes, each raw original input trace is read once again and transformed to the Gabor domain.

- Hyperbolic smoothing is applied to the Gabor magnitude spectrum, but the Q-array is not re-estimated. All spectral arrays are re-estimated as described for the second pass and summed into the *iterated estimate* arrays (previously zeroed). (The *iterated estimate* spectra are obtained from the *current estimate* spectra and the current trace residual spectra using the same arithmetic described for the second pass.)

- A deconvolution operator is assembled for the trace by multiplying magnitude spectra retrieved from the *current estimate* magnitude spectra arrays corresponding to source, receiver, and offset locations for the current trace and multiplying by the Q-array for the current midpoint location.

- The operator is stabilized by addition of a stability factor and converted (optionally) to minimum phase.

- The complex Gabor spectrum of the current trace is divided by the complex spectrum of the deconvolution operator.

- The trace is reconstructed from its modified Gabor spectrum and output from the algorithm.

- Further iterations proceed as above, with the current *iterated estimate* spectra replacing the *current estimate*, and so forth.

From the above description of the algorithm it can be seen that it differs in two ways from that described by Montana et al. First, provision has been made to include source-receiver offset as a coordinate for decomposition of the deconvolution operator. In the current formulation, the contribution to the offset-dependency is assumed to come from the *residual* Gabor magnitude spectrum, after removal of the Q-function. The offset dependency could easily be introduced into the Q-function instead, however, and this is still an open research question. Second, provision has been made to iterate the estimation of the various contributions to the deconvolution operator. ProMAX provides an easy way to accomplish this by allowing the input data to be read more than once, merely by specifying a parameter in the 'Disk data input' process. The new **gabor_sc** module expects the data to be read two or more times, and uses the trace header 'disk_iter', which is set by the data reading process, to determine the pass to which a current trace belongs. If the data are read twice only, the set of output traces will have been deconvolved using operators constructed from the first pass estimates of the source, receiver, and midpoint magnitude spectra. If the data are read three times, however, two sets of traces are output. The first of these will be the input traces deconvolved with the first pass estimates, and the second set will be the same traces deconvolved with operators constructed from the iterated magnitude spectra. If iteration proves to be of value, further iteration, and corresponding sets of output traces, can be invoked simply by adding more passes through the 'Disk data input' operation.

EXAMPLES

To illustrate the operation of the **gabor_sc** algorithm, we look at two examples: first the model data set, provided by Mike Perz (2005) from Divestco, which contains widely varying amounts of coherent and random noise, and which was used to induce phase instability in the existing ProMAX Gabor deconvolution module (Henley et al 2006); then the Blackfoot 2D data, a well-known field data set often used for algorithm testing.

The Perz model

In 2006, we used the Perz Model (Perz et al, 2005) to illustrate the drawbacks of single trace deconvolution (Henley et al, 2006). This model is well-suited to deconvolution testing because it consists of a real reflectivity sequence with Q effects applied in a known fashion. Furthermore, it has a coherent noise train added to each shot gather to simulate shot-generated noise, and varying amounts of broadband white noise added randomly to traces within each shot gather to simulate wind noise on the geophones. We determined in 2006 that the single trace derive-and-apply mode of Gabor deconvolution does the best job on each individual trace within a gather, in the sense that the individual traces are as white as possible within the constraints of the noise and/or stability factor. However, this means that when doing minimum phase deconvolution, the low-noise traces, which are whitened more than the noisy traces, exhibit event arrival times which are significantly earlier than the corresponding events on noisy traces. Stacked traces composed of varying blends of clean and noisy traces will thus exhibit event phase which varies from trace to trace, depending upon the particular blend of clean and noisy traces which make up the stack. We also showed that deriving a single operator for each shot ensemble and applying it to all the traces in the ensemble largely eliminates this problem, at the expense of some bandwidth in the stack trace.

Figure 1 shows a raw shot gather selected from the Perz data set. The same shot appears in Figure 2 after application of the standard ProMAX Gabor deconvolution algorithm in ensemble mode, where the Gabor magnitude spectrum summed over all the traces in the ensemble are used to derive a single operator to apply to the entire gather, and in Figure 3 after application of the standard ProMAX Gabor deconvolution in single trace mode. As noted above, the ensemble average deconvolution results are narrower in band, but more stable in phase than the single trace results, especially for the deepest events, which are most affected by Q attenuation. The result, for the same shot gather, of applying the **gabor_sc** algorithm, which averages over shot, receiver, and common offset ensembles, is shown in Figure 4. Clearly, these results are slightly broader in band and less noisy than the ensemble average shown in Figure 3; and they are narrower in band, but more stable in phase than the results shown in Figure 2. For these model data, there was no offset-dependent factor incorporated into the model, so we expect no particular effect from deriving and applying an offset-dependent contribution to the deconvolution operator. The differences observed between Figure 4 and the other deconvolution results should be due almost entirely to source and receiver ensemble averaging. For the sake of interest, Figure 5 shows the result of allowing the **gabor_sc** algorithm to iterate the decon operator estimates once. The differences between this image and that in Figure 4 are quite subtle, but the image in Figure 5 is slightly broader in band, and some of the fainter shallow reflections are slightly more visible against the background noise…an encouraging result.

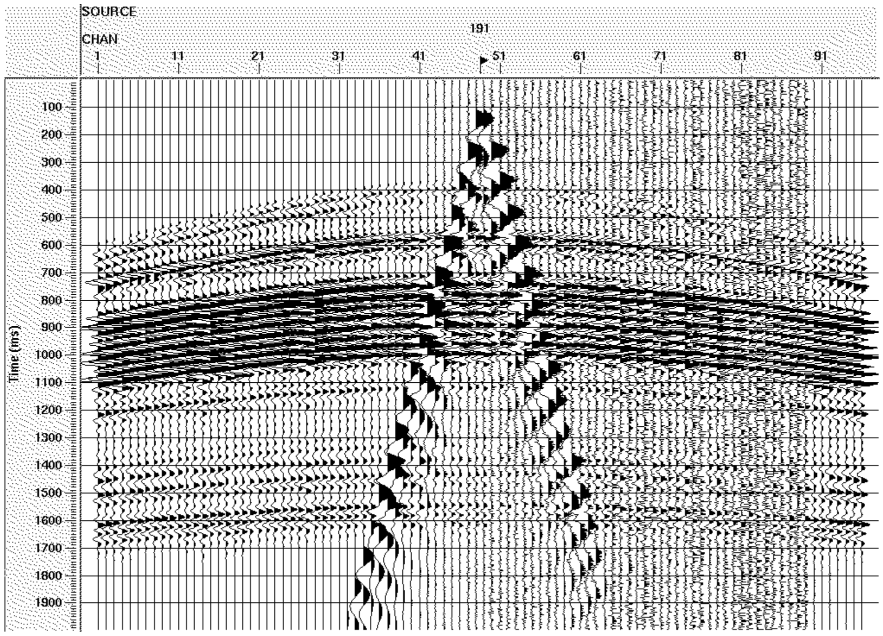

Perz model—raw shot gather

FIG. 1. Typical shot gather from Mike Perz' model, which contains coherent noise in the form of a cone of ground roll and random noise whose level varies randomly over receiver stations.

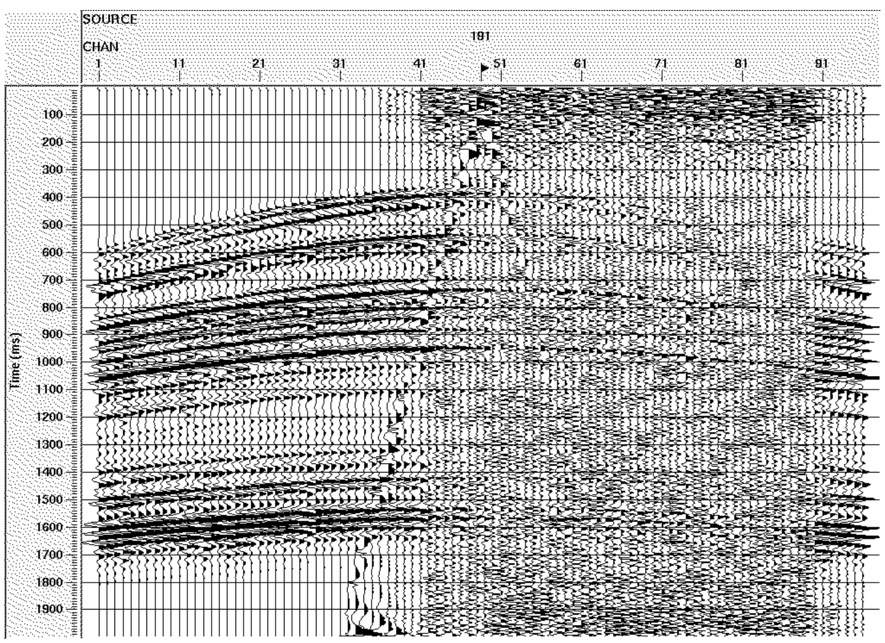

Perz model—Gabor 2: ensemble average operator

FIG. 2. The shot gather in Figure 1 after application of the ProMAX version of Gabor2 in the ensemble average mode, where an operator is derived from the average Gabor spectrum for the whole gather and applied to each individual trace.

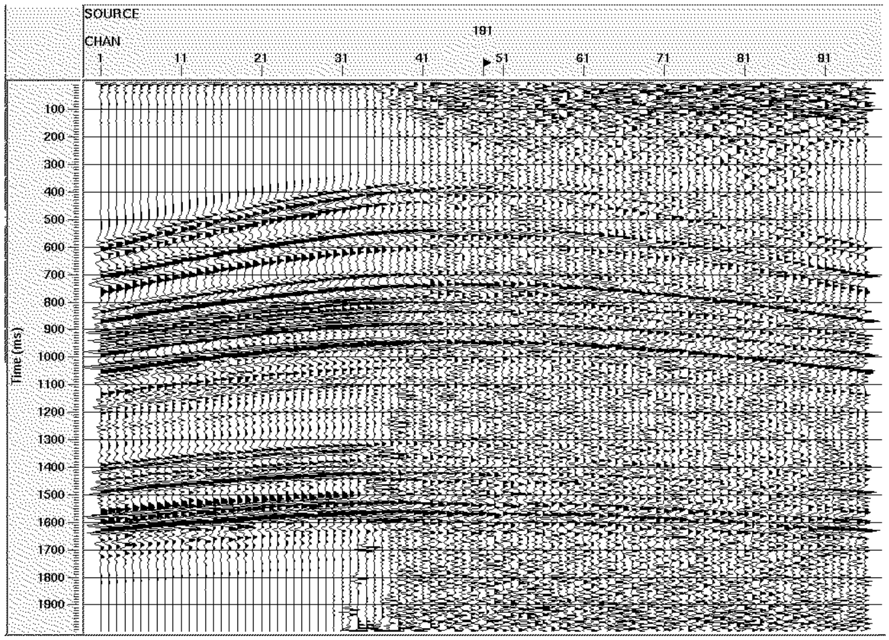

Perz model—Gabor 2: single trace operator operator

FIG. 3. The shot gather in Figure 1 after application of the ProMAX version of Gabor2 in the single trace mode, where an operator is derived for each trace individually and applied only to that trace. The less-noisy traces are whitened much more than the noisy ones in this mode. Their reflection event times are also shifted shallower in time by the minimum phase constraint.

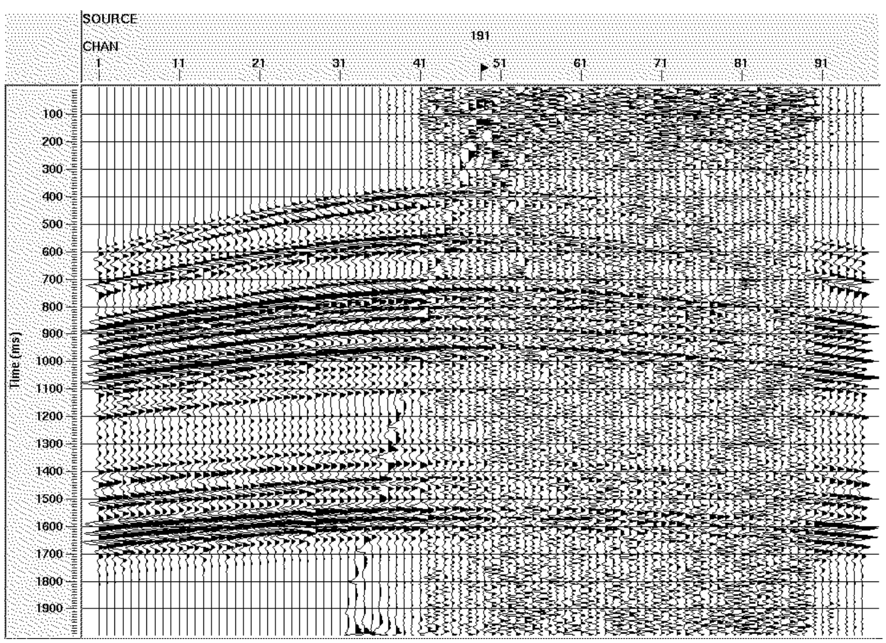

Perz model—Gabor SC surface consistent decon operator

FIG. 4. The shot gather in Figure 1 after application of the new ProMAX version of **gabor_sc**. Here, the operator for each trace is composed of components averaged over shot, receiver, and offset.

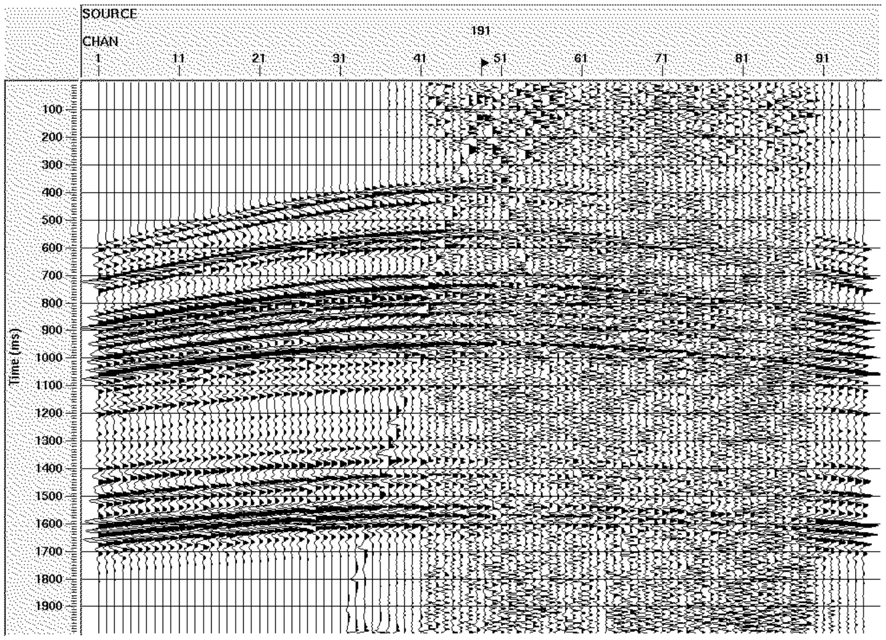

Perz model—Gabor SC surface consistent decon operator second iteration

FIG. 5. The shot gather in Figure 1 after the second iteration of the **gabor_sc** module. The components of the decon operators have been iterated as described in the text.

Blackfoot

Figure 6 shows a typical shot gather from the vertical component of the Blackfoot 3C 2D data set. When we examine all the gathers on this line, it becomes evident that for this data set, traces at a given common offset often have more in common than traces in a common shot or common receiver, so we expect offset-dependence to play more of a role in deconvolving these data. Figure 7 shows the ensemble average mode of Gabor deconvolution, where the ensemble was again the shot record, while Figure 8 illustrates the single trace mode Gabor deconvolution.

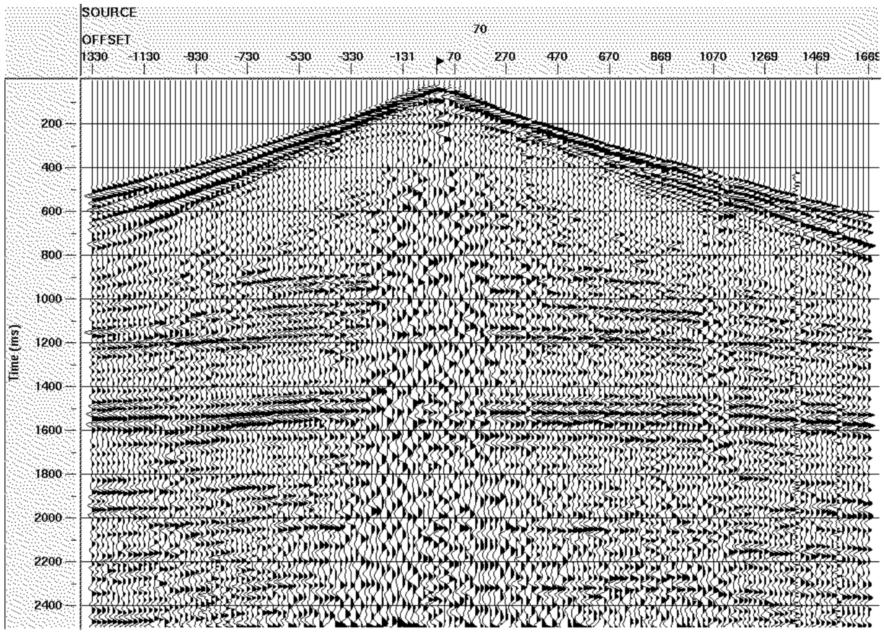

Blackfoot shot gather—bandpass only

FIG. 6. Typical vertical component shot gather from the Blackfoot 2D 3C survey, after bandpass filter only.

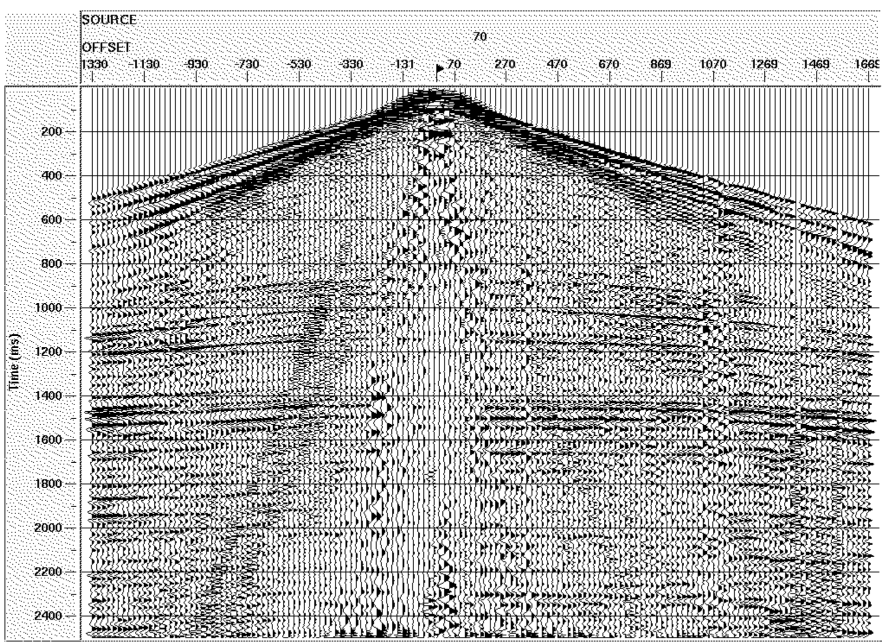

Blackfoot shot gather—Gabor 2 ensemble average

FIG. 7. Blackfoot shot gather from Figure 5 after application of ProMAX version of Gabor2 in the ensemble average mode.

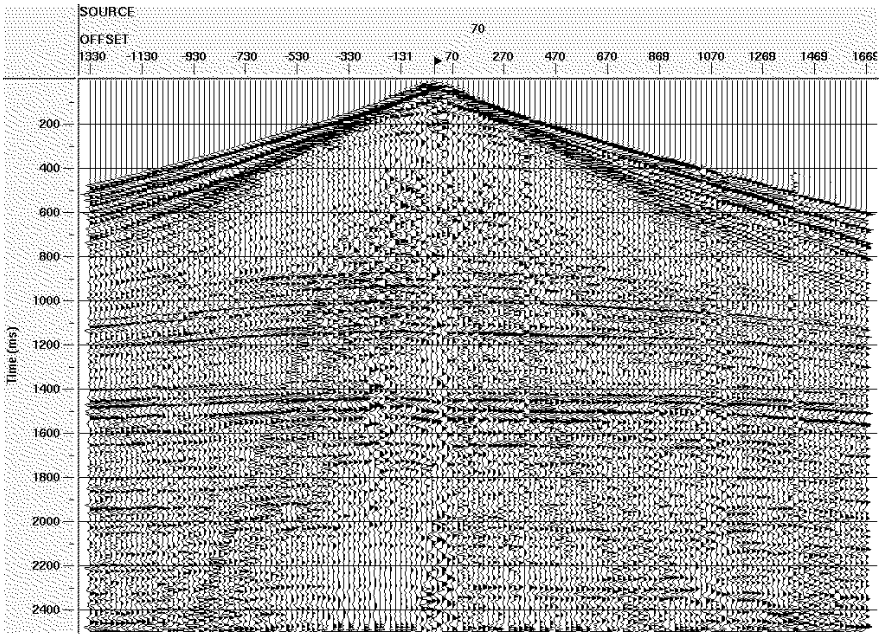

Blackfoot shot gather—Gabor 2 single trace mode

FIG. 8. Blackfoot shot gather from Figure 5 after application of ProMAX version of Gabor2 in the single trace mode.

For comparison, Figure 9 shows the results from **gabor_sc**. Differences between the several modes of deconvolution are fairly subtle, probably because these data are relatively clean, with no particularly pronounced shot or receiver oriented effects. Nevertheless, the results in Figure 9 seem to show characteristics intermediate between those in Figures 7 and 8. Perhaps most noteworthy is the differing performance of the deconvolution algorithms in enhancing reflections that are buried beneath the coherent noise on the inner offsets between about 800 and 1800 ms. The single trace mode has clearly done the best job here while the shot-ensemble mode has barely revealed these reflectors. The surface-consistent mode seems slightly better than the shot-ensemble mode.

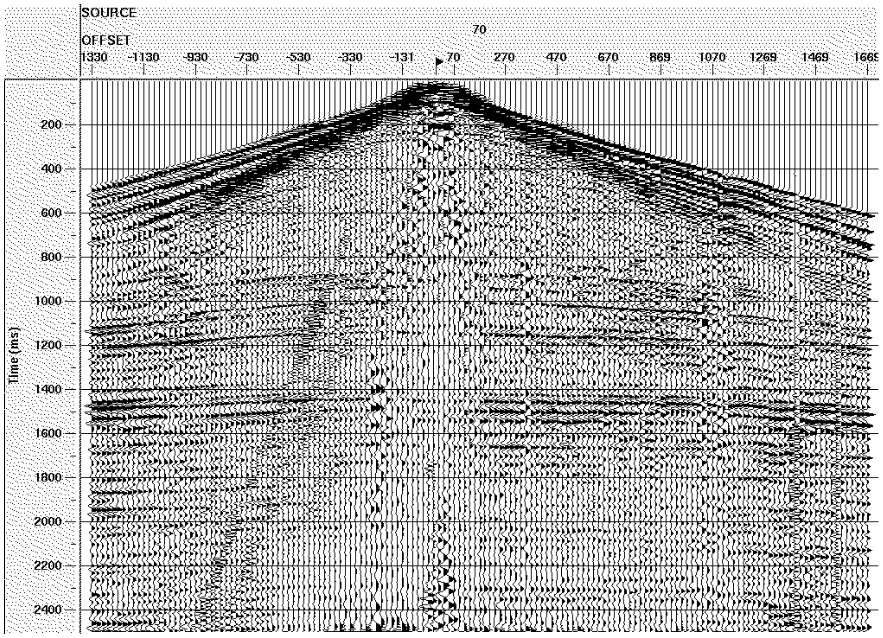

Blackfoot shot gather—Gabor SC first pass

FIG. 9. Blackfoot shot gather from Figure 5 after application of ProMAX version of **gabor_sc** using the first estimate for source, receiver, and offset dependent wavelets.

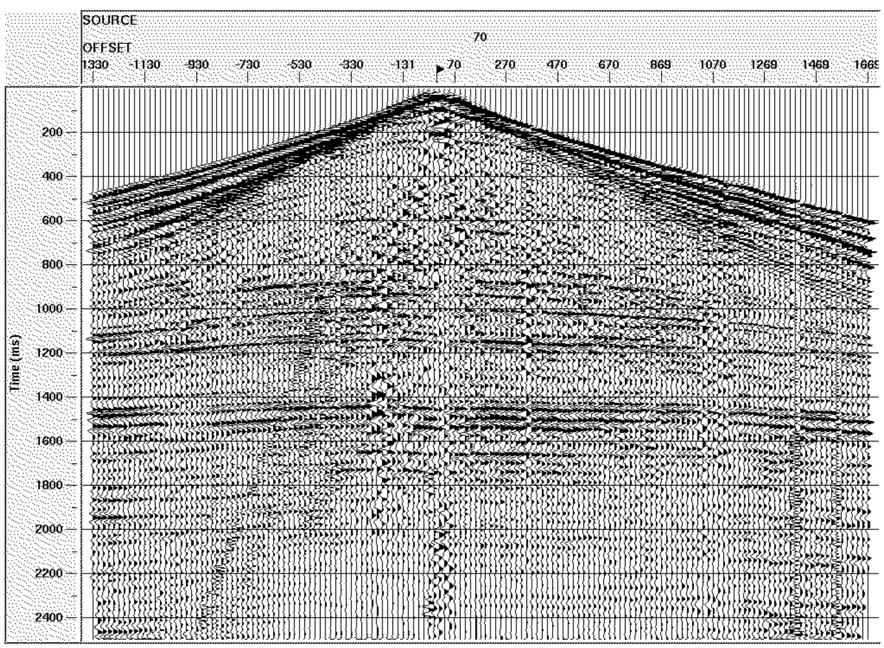

Blackfoot shot gather—Gabor SC second iteration

FIG. 10. Blackfoot shot gather from Figure 5 after application of ProMAX version of **gabor_sc** using the second, iterated estimates for source, receiver, and offset dependent wavelets.

As a further test of the iteration in the algorithm, Figure 10 shows the results of iterating the estimation of surface-consistent deconvolution operators. It is interesting to note the improved strength and continuity of several of the reflection events on this gather, although the bandwidth does not appear to increase significantly over that in Figure 9. Although this result begins to resemble the single trace mode deconvolution in Figure 8, intuitively, we would not expect its bandwidth to be quite as great, since all the component magnitude spectra used to construct the deconvolution operators for the results in Figures 9 and 10 are averaged over many input spectra. What we do expect, however, is for the event phase to be more stable in the presence of noise on the input traces.

DISCUSSION

We are in the very early stages of testing the ProMAX version of surface-consistent Gabor deconvolution; so we have little to say at this point regarding its preferred use. Neither data set used to illustrate **gabor_sc** in this report was particularly appropriate for showing the advantage of surface-consistency, since neither set contains significant near-surface effects attributable to specific shot or receiver locations. One advantage of the new **gabor_sc** algorithm, with the addition of offset-dependence, is the ability to forego the customary application of linear moveout before decon, followed by moveout restoration afterwards (an attempt to emulate trace gating on input gathers). In the new algorithm, the offset-dependence can absorb any differences due to first arrival variation with offset.

We intend to test **gabor_sc** on various data sets to try to establish its advantages and disadvantages. In addition, we have the ability to test various arithmetic ways of apportioning the variability in the deconvolution operator to source, receiver, offset, or midpoint, and to test full iterative estimation of the deconvolution operator contributions as described in the algorithm above.

The **gabor_sc** algorithm is being released to sponsors in this year's software, but it should be understood that this is very much a *beta* version, subject to bugs and to frequent future changes. The documentation is included in the appendix to this report.

ACKNOWLEDGEMENTS

The authors gratefully acknowledge CREWES sponsors for continuing financial support and CREWES staff for continuing technical assistance.

REFERENCES

Margrave, G.F., and Lamoureux, M.P., 2001, Gabor deconvolution: CREWES 2001 research report, **13**.

Margrave, G.F., Lamoureux, M.P., Grossman, J.P., and Iliescu, V., 2002, Gabor deconvolution of seismic data for source waveform and Q correction: 72nd Ann. Internat. Mtg. Soc. Expl. Geophys., Expanded abstracts, 2190-2193.

Margrave, G.F., and Lamoureux, M.P., 2002, Gabor deconvolution: 2002 CSEG Annual Convention, Expanded abstracts.

Margrave, G.F., Linping Dong, Grossman, J.P., Henley, D.C., and Lamoureux, M.P., 2003, Gabor deconvolution: extending Wiener's method to nonstationarity: CREWES 2003 research report, **15**.

Montana, C., Margrave, G.F., and Henley, D.C., 2006, Surface consistent Gabor deconvolution: CREWES 2006 research report, **18**.

Perz, M., Mewhort, L., Margrave, G.F., and Ross, L., 2005, Gabor deconvolution: real and synthetic data experiences: 2005 CSEG Annual Convention, Expanded abstracts.

APPENDIX

Gabor surface consistent—Promax module documentation

This module applies Gabor Deconvolution in a surface-consistent manner to a panel of seismic traces, trace-by-trace. The algorithm is a time-varying deconvolution whose operator adapts to the characteristics of the particular data captured by a time-overlapped set of windows. Gabor surface consistent differs from its predecessors in that the decon operator derived from the first pass of a trace is split into a source wavelet component, receiver wavelet component, offset-dependent component, and Q-factor component. These components are stored according to their source, receiver, offset, and midpoint trace header values, respectively. Subsequent trace decon operators are summed into these source, receiver, offset, and midpoint arrays, also according to their associated trace header values. After all the traces in a line are read, the program begins a second pass through the trace file. During the second pass, averaged decon operator components are retrieved from the respective arrays according to matching trace headers, combined into a single decon operator for each trace, the phase computed (either zero or minimum phase) and the composite decon operator applied to the trace. Currently, the wavelet averages are mean averages, and the composite wavelet is the product of source, receiver, and offset average wavelets.

An experimental extension of the routine uses the second pass through the data set to iterate the estimated source, receiver, and offset wavelet arrays by dividing products of the first pass estimates for source, receiver, and offset into the composite wavelet estimate from the second pass to obtain new estimates for source and receiver wavelets. These estimates are summed into new source, receiver, and offset wavelet arrays and accumulated for the whole line. A third pass through the data then retrieves the iterated source and receiver wavelets for each trace, as well as the Q-array and builds a composite deconvolution operator for each trace. In the current arrangement, traces are output both from the second pass and the third pass, thus providing two versions of the surface-consistent deconvolution.

This current, experimental version of surface-consistent Gabor decon has provision for experimenting with offset-dependence, as indicated above. Currently, the "wavelet" magnitudes extracted from the input Gabor transform after hyperbolic smoothing are summed into arrays indexed by source surface position, receiver surface position, and source-receiver position *difference* (equivalent to absolute offset). This means that as ideas for incorporating offset-dependence are available, the offset-summed wavelet estimate will be immediately available for spectral arithmetic within the decon operator computation.

Updates

This version of Gabor surface consistent is the first and has not been thoroughly tested. This is definitely a ‘beta’ version.

Theory

Gabor deconvolution is based on the Gabor Transform, which is a way to analyse a seismic trace for time-varying spectral characteristics. Because this transform explicitly captures the nonstationary behavior of a seismic trace, it constitutes a natural basis for its deconvolution. The deconvolution is applied in the frequency domain by performing a complex division of the Gabor Transform by the derived deconvolution operator. The time-dependency of the resulting array is removed by summing over the time-gate dimension of the array.

Surface-consistency is invoked for deconvolution anytime it is considered that the "wavelet" derived for each trace has particular features attributable to either the source location or receiver location, or both. Surface consistent arithmetic thus leads to more robust estimates for the parts of the deconvolution wavelet peculiar to its raypath endpoints.

Usage

This version of Gabor deconvolution is intended for application to pre-stack data, since it specifically requires certain trace headers for its proper functioning. The input data may be source gathers, receiver gathers, or CDP gathers.

The program must estimate buffer requirements in the initialization phase and thus requires the existence of a database for any line submitted, from which it finds the total number of shots, receivers, and CDPs. Any line for which there is no pre-existing database must have one created using the 'Extract database files' function following the 'Disk data input'.

In order for the program to function properly, the 'Disk data input' which precedes it must have the "Read data multiple times" option set to "yes", and the number of iterations immediately below it set to either '2' or '3'. If the data set is read twice, the output from the program will be the input traces deconvolved with the first pass estimated source, receiver, and offset wavelets. If the data set is read three times, the output will consist of the input traces first deconvolved with the source, receiver, and offset wavelets from the first pass, then the same input traces deconvolved with the source, receiver, and offset wavelets estimated by iteration. The two complete data sets are distinguished from one another by the trace header 'DISKITER', which is set to '2' for the traces deconvolved by the first wavelet estimates and '3' for the traces deconvolved by the iterated wavelet estimates. This trace header thus allows the two output data sets to be written as separate files, using, for example, an 'IF'--'ENDIF' loop to test the value of 'DISKITER'.

Parameters

Half-width of the analysis/synthesis window--This is the half-width in seconds of the Lamoureux window functions used for analysis and synthesis of the data traces. Since the Lamoureux functions have a finite width between their zero amplitude points, the half-width is half the distance between the zero amplitude points, not the 1/e amplitude points as in Gaussian functions.

Window increment factor--Lamoureux windows are properly overlapped and normalized if the start point (zero amplitude) of one window coincides with the centre of the preceding window, and the end point (also zero amplitude) coincides with the centre of the succeeding window. In order to keep this proper window normalisation, the increment between windows may be decreased only by applying additional properly overlapped sets of windows, offset from the original windows by increments evenly divisible into the original window width. Hence an increment factor of 2 generates an additional overlapped set of windows, offset from the original set by one fourth of the window width; an increment factor of 3 generates two additional overlapped sets of windows, the second and third offset from the first by 1/6 and 1/3 of the window width, respectively, and so forth. Proper normalisation is maintained by dividing the windowed data by the window increment factor, which is equal to the total number of unity-normalised sets of overlapped windows used to sample the data. Using a value greater than one appears to stabilise the result, particularly on noisy data.

Factor to extend window before FFT--This factor is applied to the window length to determine the actual length of the FFT used to analyze the windowed trace segment. The trace segment is extended by this factor, then further extended to the next largest power of two prior to the FFT.

Pad input traces before windowing--This is a switch parameter which determines whether or not the input traces are padded before windowing, to diminish end effects. If this switch is set to true, the following parameter is used to determine the length of pad to be added to both beginning and end of the traces. The pad values are random noise whose level is set to -300 dB of the rms amplitude level of the current trace, in order that windows never encounter an all-zero trace segment.

Fraction of window width for trace padding--If the switch above is set to true, this parameter is used to determine the number of pad values to append to either end of the trace. The recommended value is more than half a window width, to move end effects off the visible seismic trace.

Slope exponent for Lamoureux window function--This integer is used as an exponent in the computation of the values of the Lamoureux window. Its default value of 2 is a safe choice. Larger values can lead to window artifacts under conditions of high noise, low signal level, and small window overlap.

Application exponent for analysis window--Prior to being applied to the input trace, the values of the analysis window function are raised to this power (actually a root, since the value must be .LE. 1.0). The values of the synthesis window function are then raised to the complementary power (1.0 minus application exponent). A value of 0.5 applies a square root window to both analysis and synthesis; one applies a full strength analysis window and no synthesis window; zero applies no analysis window function and a full strength synthesis window.

Choose type of spectrum for wavelet estimate--This parameter chooses whether the Fourier Transform or the Burg algorithm is used to compute the spectral magnitudes used to construct the deconvolution operator. The Burg algorithm is somewhat slower than the FFT, if used with many coefficients.

Number of coefficients for Burg spectrum--This parameter only appears if Burg spectra are used in the decon operator. In general, the more coefficients, the more detail the Burg spectrum contains. Since the spectra are smoothed to obtain the decon operator, a small number of coefficients (3-5) will often be more effective than a larger number (10) and will run somewhat faster as well. Using a small coefficient number is similar to applying more smoothing, so the spectral smoothing parameter below can be smaller in this case.

Choose minimum or zero phase deconvolution--While a minimum phase decon would be the norm here, zero phase can be chosen, and it takes less time to construct the operator.

Choose corridor width of hyperbolic smoothing in Hz-sec--This parameter determines how much smoothing occurs in the constant time-frequency method. A wide corridor applies more smoothing, forcing more of the time-dependency into the subsequent wavelet estimation.

Wavelet smoothing window length in seconds--Determines the number of spectral magnitude points to be smoothed in time.

Begin time in seconds for Q estimation--This parameter determines the time before which estimated Q-factor is constant.

End time in seconds for Q estimation--This parameter determines the time after which estimated Q factor is constant.

Stability factor for spectral division operations--This parameter determines the fraction of the maximum spectral magnitude to be added to all decon operator spectral magnitudes to prevent any division by zero. The default value is a safe option.

References

G. Margrave, M. Lamoureux, D. Henley C. Montana